Hindawi
Geofluids
Volume 2021, Article ID 3610207, 8 pages
https://doi.org/10.1155/2021/3610207

WILEY | Hindawi

Research Article

Comparison of Foamy Oil Behaviour between Shallow and Middepth Heavy Oil Reservoirs in the Orinoco Belt

Xingmin Li, Changchun Chen, Zhangcong Liu, Yongbin Wu, and Xiaoxing Shi

Research Institute of Petroleum Exploration & Development, PetroChina, Beijing 100083, China

Correspondence should be addressed to Xingmin Li; lxingmin@petrochina.com.cn

Received 19 June 2021; Accepted 4 August 2021; Published 11 November 2021

Academic Editor: Xiaofei Sun

Nowadays, extra heavy oil reservoirs in the Orinoco Heavy-Oil-Belt in Venezuela are exploited via cold production process, which present different production performance in well productivity and primary recovery factor. The purpose of this study is to investigate the causes for such differences with the aspect of foamy oil mechanism. Two typical oil samples were adopted from a shallow reservoir in western Junìn region and a middepth reservoir in eastern Carabobo region in the Belt, respectively. A depletion test was conducted using 1D sand-pack with a visualized microscopic flow observation installation for each of the oil samples under simulated reservoir conditions. The production performance, the foamy oil behaviour, and the oil and gas morphology were recorded in real time during the tests. The results indicated that the shallow heavy oil reservoir in the Belt presents a weaker foamy oil phenomenon when compared with the middepth one; its foamy oil behaviour lasts a shorter duration with a smaller scope, with bigger bubble size and less bubble density. The difference in foamy oil behaviour for those two types of heavy oil reservoir is caused by the difference in reservoir pressure, solution GOR, asphaltene content, etc. Cold production presents obvious features of three stages under the action of strong foamy oil displacement mechanism for the middepth heavy oil reservoir, which could achieve a more favourable production performance. In the contrary, no such obvious production characteristics for the shallow heavy oil reservoir are observed due to weaker foamy oil behaviour, and its primary recovery factor is 9.38 percent point lower than which of the middle heavy oil reservoirs.

1. Introduction

Extra heavy oil in the Orinoco Heavy-Oil-Belt in Venezuela nowadays is exploited via solution gas drive process or so-called cold production and presents some certain foamy oil behaviour [1, 2]. Foamy oil flow describes a form of two-phase oil-gas flow in porous media in which the gas phase remains partially or completely dispersed in the oil, when the pressure drops below the bubble point pressure (P_b) and above the pseudo bubble point pressure (P_{sb}) during depletion process, while in conventional oils, the gas rapidly coalesces into large bubbles and forms immediately a separate and distinct gas phase. The delayed free gas production maintains a higher reservoir pressure and thus delivers greater primary recovery comparing to conventional heavy oil reservoirs. According to the structural and sedimentary characteristics, the Orinoco Belt is divided into four regions from west to east, namely, Boyacá, Junìn, Ayacucho, and Carabobo. Different reservoirs in the Orinoco Belt vary in well productivity and primary recovery factor, due to difference in reservoir buried depth, reservoir properties, crude oil viscosity, original dissolved gas oil ratio (GOR), and also due to the difference in foamy oil performance, that is, strong or weak foamy oil behaviour. The formation and strength of foamy oil depend on many factors, including temperature, GOR, pressure and pressure depletion rate, pore structure, permeability, crude oil viscosity, and oil composition [3–9]. In the Orinoco Belt, the buried depth of the main oil-bearing formations is approximate 300-500 m in Boyacá and Junìn regions, which is classified into shallow reservoir type, and 800-1200 m in Ayacucho and Carabobo regions, which is classified into middepth reservoir type. Most of the literatures on foamy oil studies for the Orinoco Belt focus on the eastern Ayacucho and Carabobo regions, and the studies indicate that foamy oil drive mechanism plays a significant role for cold production in those two regions, and

the cold production performs favourably [10, 11]. The averaged well productivity is more than 200 t/d, and the primary recovery factor can reach 10-12% generally. However, in some shallow heavy oil reservoirs in Junìn region, the cold production performs relatively poorly, with an averaged well productivity less than 70 t/d and a primary recovery factor of no more than 6%. Study on foamy oil behaviour in those heavy oils is rare. It is the purpose of this paper to investigate the foamy oil behaviour in such shallow heavy oils in western Junìn region and compare with middepth heavy oils in the eastern region thus to deeply understand the reason why the cold production performs unfavourably and provide the basis for seeking strategies to improve the productivity. Two typical oil samples are adopted for the comparison studies; one is from a shallow reservoir T in western Junìn region, and the other is from a middepth reservoir M in eastern Carabobo region, respectively.

2. Experiments

2.1. Experimental Materials. The basic reservoir and fluid parameters for reservoir T in Junìn region and reservoir M in Carabobo region are listed in Table 1.

The degassed crude oil samples from reservoir T and reservoir M were used as the dead oil. A mixture of CH_4 and CO_2 was used as the solution gas, in which the mole fraction of CH_4 was 90% in reservoir T and 87% in reservoir M, respectively. The live oil samples were prepared through a high temperature and high-pressure cylinder. The formation brine contents of Ca^{++}, Mg^{++}, Fe^{++}, Na^{++}, HCO_3^-, and Cl^- are 76, 29, 0.2, 3967, 2782, and 4710 mg/l, respectively, for reservoir T, and 247, 152, 92, 7125, 2800, and 10360 mg/l, respectively, for reservoir M. The purity of methane and CO_2 adopted in the experiments are 99.99%. The sand-packs were made up of clear quartz sand with grain size of 212 to 355 μm.

2.2. Experimental Setup. The experimental setup is mainly comprised of a fluid injection system, a reservoir simulation system, a visualized microscopic flow observation system, an oil and gas separation and metering system, and a data acquisition and control system. Figure 1 shows the schematic of the experimental setup.

The fluid injection system is mainly composed of a constant-pressure and constant-flux pump, two intermediate vessels, and a heating sleeve. The vessels are connected with the pump, which are used to saturate formation water and live oil into the core. The reservoir simulation system mainly includes a long core holder, a plunger pump, and a thermostatic box. The core holder can fill the core with a diameter of 2.5 cm and a length of 100 cm, with six pressure measuring points. The visualized microscopic flow observation system mainly includes a high-temperature and high-pressure visualized observation window, a camera, and a light source. A specially designed visualized window is connected to the outlet of the long core holder, which can withstand a pressure of 15 MPa and a temperature of 150°C. The foamy oil phenomenon and the oil and gas morphology in the visible window can be recorded in real time by the high-definition camera. The data acquisition and control system mainly include a computer, a back-pressure valve, and a nitrogen cylinder. The pressure in the long core and the pressure drop rate in the depletion process can be controlled by the back-pressure valve. The computer automatically records the pressure values of each pressure measuring point every minute. According to the core pressure, the plunger pump is automatically controlled to adjust the confining pressure, and the difference between the core pressure and the formation stress is kept stable. The oil and gas separation and metering system mainly includes an oil and gas separation bottle, an electronic balance, a vacuum pump, and a gas measuring cylinder. The crude oil produced is measured by the electronic balance, and the volume of gas is measured by the gas cylinder.

2.3. Experimental Procedures. The experimental procedures include the following steps:

(1) *Model Preparation*. The sand-pack holder was packed with quartz sand and then evacuated for more than two hours before it was saturated with water to measure porosity. The water saturated sand-pack was then heated for 4 hours, and the system was kept at the reservoir temperature, and its permeability was measured under several water flow rates. Following this, about 7 PV prepared live oil was injected at a pressure slightly above the formation pressure to displace water, and initial oil saturation was measured. During the process, the produced GOR was measured at regular intervals to examine the uniform oil saturation establishment along the porous media. And then, the core was stabilized for 24 hours to guarantee the uniform distribution of temperature and pressure.

(2) *Primary Depletion*. The valve at the outlet end of the sand-pack was opened, and the back-pressure regulator was set on the depressurization mode to initiate the depletion process at a certain pressure depletion rate. The pressure of each pressure port was recorded vs. time by the computer. The oil and gas production rates were measured continuously. The depletion was stopped when the pressure declined to a certain value. Meanwhile, the foamy oil phenomenon and the oil and gas morphology in the visible window were recorded in real time by the high-definition camera.

3. Results and Discussion

Two sets of 1D sand-pack depletion test were conducted for reservoir T and reservoir M, respectively. The experimental sand-pack parameters are listed in Table 2, and the depletion production data are listed in Table 3.

The visualized gas bubble distribution statistical results are in Tables 4 and 5 for test 1 and test 2, respectively.

For test 1, the oil production rate, Cum. oil production, and oil recovery degree curves are shown in Figure 2(a); the produced GOR and Cum. gas production curves are shown in Figure 2(b); the pressure variation vs. time at different 6 pressure measuring points (P1-P6) are shown in

Table 1: Basic reservoir and fluid parameters in reservoir T and reservoir M.

	Reservoir T	Reservoir M
Region	Junìn	Carabobo
Reservoir depth, m	415	870
Reservoir pressure, MPa	4.2	8.7
Reservoir temperature, ˚C	45.6	53.4
Oil zone thickness, m	6-67	27-77
Porosity, %	33-34	30-36
Permeability, md	5000-13000	4000-6000
Oil saturation, %	83	86
Oil gravity, ˚API	7.2	7.8
Degassed oil viscosity@ Tr, cP	3,0000	1,4488
Underground oil viscosity, cP	9000	3000
Bubble point pressure, MPa	3.5	5.1
Solution gas-oil ratio, m^3/m^3	8.6	15.9
Saturates/aromatics/resins/asphaltenes, wt%	13/42/31/15	6/40/33/21

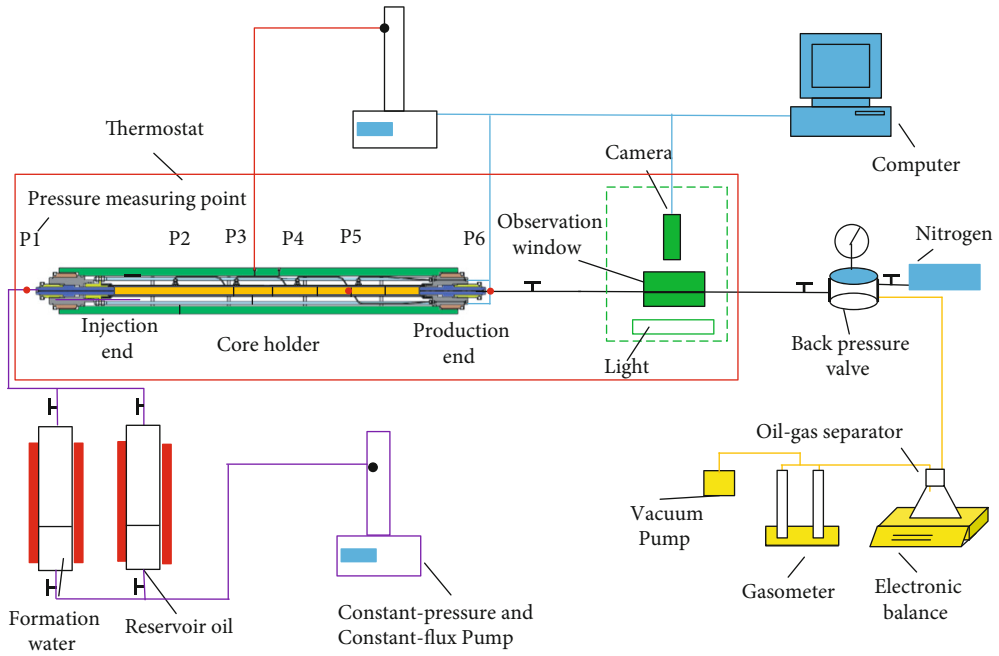

Figure 1: Schematic diagram of the experimental setup.

Table 2: Experimental sand-pack parameters.

Reservoir	Test No.	Pressure depletion rate (MPa/h)	Core length (cm)	Core diameter (cm)	Permeability (μm^2)	Porosity (%)	Oil saturation (%)
T	1	1	94	2.4	6.00	34.80	86.0
M	2	1	97	2.4	7.74	32.88	89.3

Figure 2(c); the foamy oil phenomenon and the oil and gas morphology at different pressure are shown in Figure 2(d).

For test 2, the oil production rate, Cum. oil production, and oil recovery degree curves are shown in Figure 3(a); the produced GOR and Cum. gas production curves are shown in Figure 3(b); the pressure variation vs. time at different 6 pressure measuring points(P1-P6) are shown in Figure 3(c). The foamy oil phenomenon and the oil and gas morphology at different pressure are shown in Figure 3(d).

3.1. Determination of Pseudo Bubble Point Pressure. Due to the entrainment of gas in the oil phase, the foamy oil presents a pseudo bubble point pressure (P_{sb}), which is lower than the thermodynamic equilibrium P_b. P_{sb} value relates

Table 3: Sand-pack depletion experimental results.

Test No.	Cum. oil production (g)	Max. oil production rate (g/min)	Cum. gas production (cm^3)	Recovery factor (%)	Pseudo bubble point pressure (MPa)
1	15.66	0.24	329.69	10.43	0.41
2	30.95	0.34	1498	19.81	2.12

Table 4: Visualized gas bubble distribution in test 1.

Pressure (MPa)	Bubble quality	Bubble density (per cm^2)	Max. bubble diameter (mm)	Average bubble diameter (mm)	Bubble shape
3.73	0	0	/	/	/
3.39	9	1.99	0.44	0.25	Circle
2.79	17	3.77	0.55	0.30	Circle
2.22	13	2.88	0.81	0.33	Circle
1.71	24	5.32	1.00	0.34	Circle
1.22	92	20.39	0.89	0.33	Circle
1.15	86	22.83	0.86	0.25	Circle
0.97	254	56.29	0.95	0.25	Circle
0.58	397	87.98	1.04	0.30	Circle/irregular ellipse
0.18	86	19.06	1.82	0.40	Circle/long strip

Table 5: Visualized gas bubble distribution in test 2.

Pressure (MPa)	Bubble quality	Bubble density (per cm^2)	Max. bubble diameter (mm)	Average bubble diameter (mm)	Bubble shape
5.60	0	0	/	/	/
5.00	6	1.33	0.34	0.27	Circle
4.60	42	9.31	0.53	0.25	Circle
4.08	75	16.62	0.71	0.30	Circle
3.55	223	49.42	0.73	0.22	Circle
3.41	270	59.83	0.75	0.21	Circle
3.19	341	75.57	0.91	0.26	Circle
2.65	482	106.81	0.93	0.28	Circle
2.47	570	126.32	0.98	0.29	Circle
2.25	789	174.85	0.98	0.28	Circle
2.02	456	101.05	1.41	0.30	Circle/irregular ellipse
1.66	418	92.63	1.01	0.29	Circle/irregular ellipse
1.18	363	80.44	1.03	0.30	Circle/irregular ellipse
0.79	405	89.75	3.01	0.34	Circle/irregular ellipse
0.60	382	84.65	2.14	0.33	Circle/irregular ellipse
0.56	493	109.25	2.26	0.35	Circle/irregular ellipse
0.44	315	69.81	3.17	0.40	Circle/long strip
0.31	202	77.78	5.43	0.43	Circle/long strip
0.25	187	41.44	3.27	0.47	Circle/long strip
0.10	103	22.16	6.25	0.48	Circle/long strip

to specific pressure depletion rate. Here, 1D depletion test and observed foamy oil microscopic morphology are combined to determine the P_{sb} under the test condition. For 1D depletion process, taking test 2 as an example, plotting the recovery degree and produced GOR vs. pressure clearly indicates that there exist three following different drive processes, as shown in Figure 3(a). (1) Elastic drive. When pressure is above P_b, the depletion process presents traditional

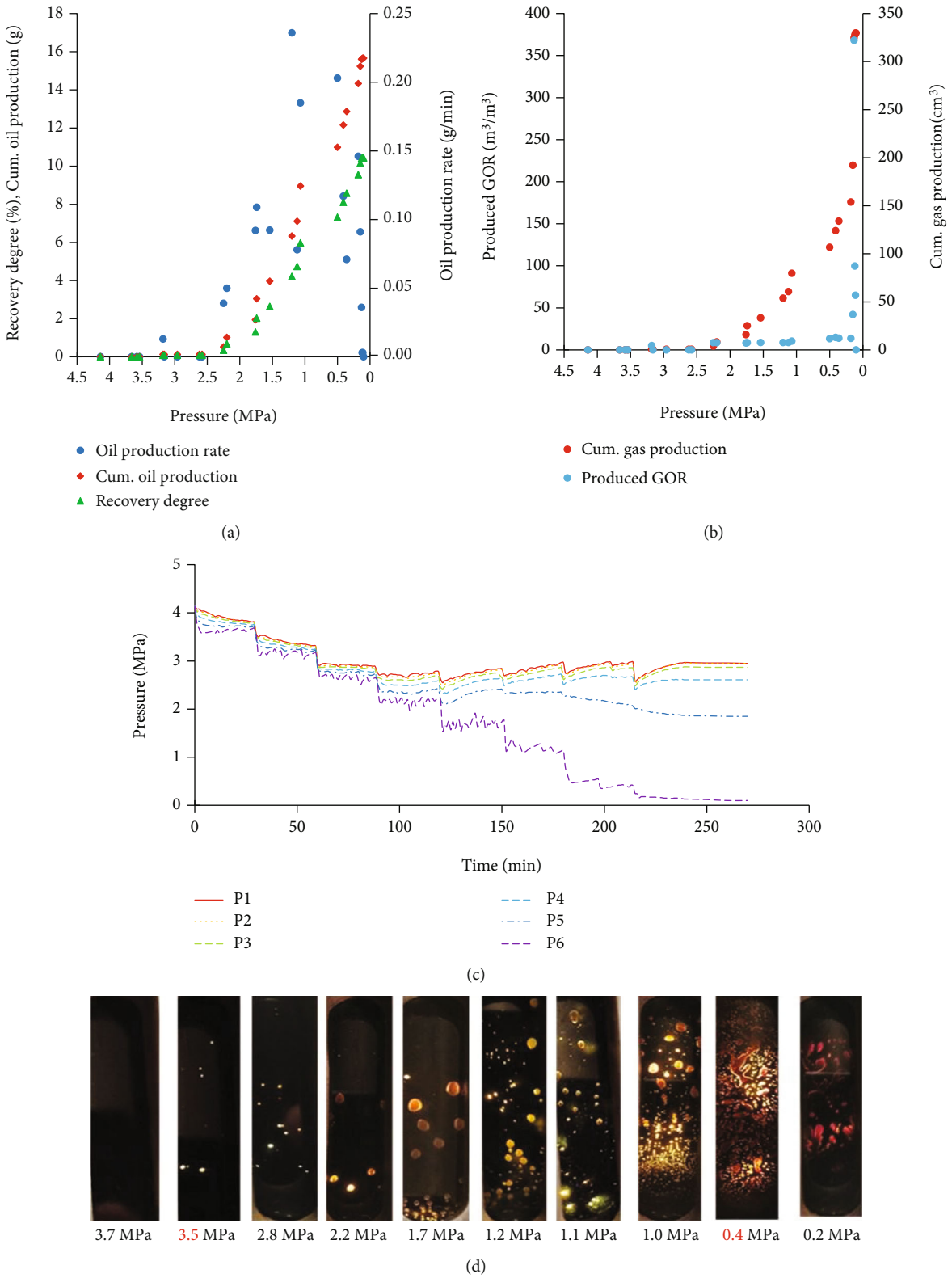

Figure 2: Experimental results of test 1: (a) oil production rate, Cum. oil production, and oil recovery degree; (b) produced GOR and Cum. gas production; (c) pressure; (d) foamy oil phenomenon and oil/gas morphology.

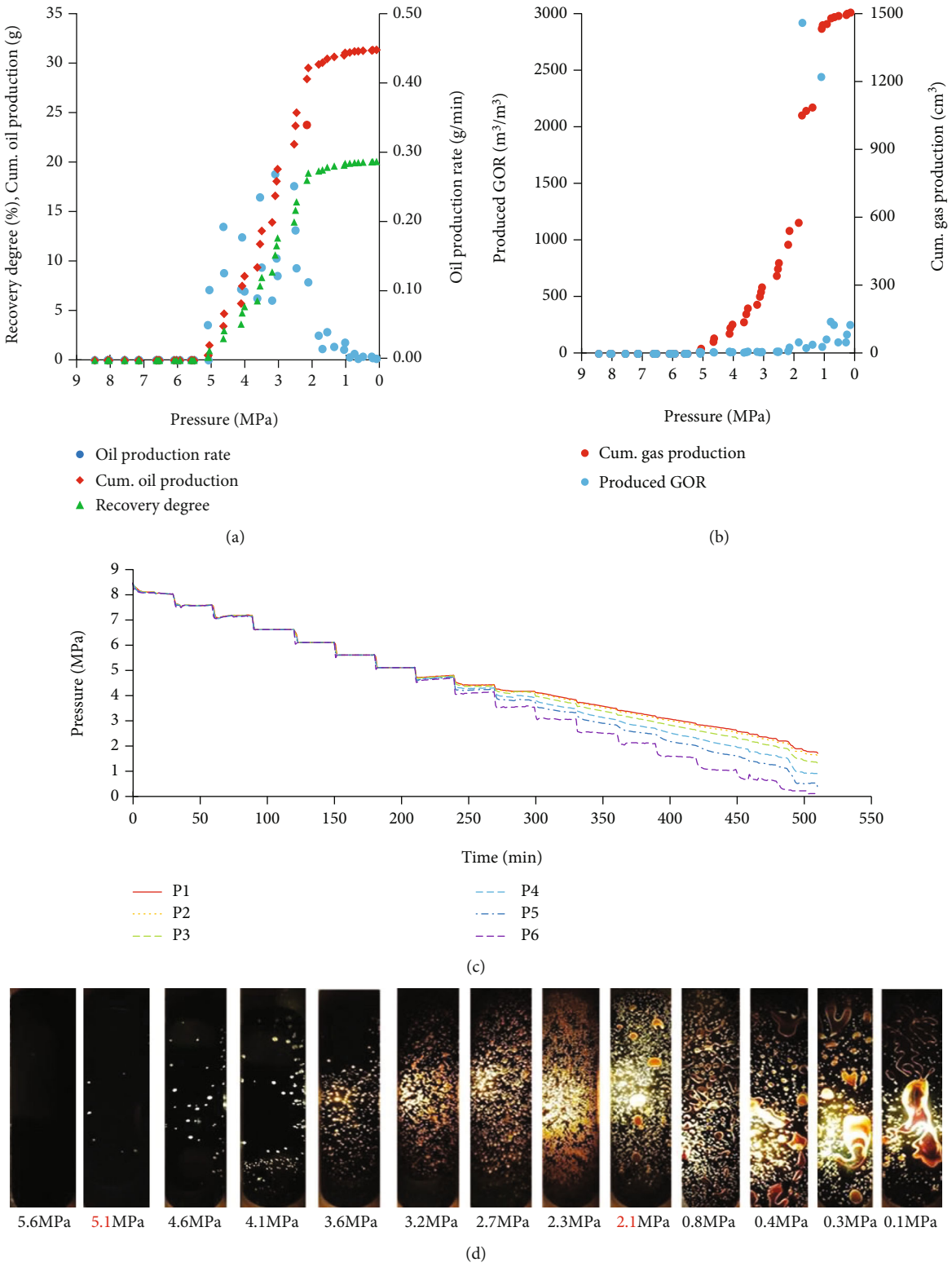

FIGURE 3: Experimental results of test 2: (a) oil production rate, Cum. oil production, and oil recovery degree; (b) produced GOR and Cum. gas production; (c) pressure; (d) foamy oil phenomenon and oil/gas morphology.

elastic drive, and the produced GOR keeps as the same as the initial GOR. (2) Foamy oil flow. With pressure drops below the P_b, the dispersed gas-in-oil flow formed and continues until the pressure is below a certain critical pressure value, and the produced GOR keeps relatively stable and a little higher than initial GOR. (3) Oil-gas two-phase flow. When

pressure drops below abovementioned critical pressure, a free mobile gas phase forms, and the process comes into traditional oil-gas two-phase flow stage, and produced GOR goes up rapidly.

The recovery factor shows approximately linear relationship against pressure for those three stages with obviously different slope. In this work, the pressure corresponding to the intersection point of the foamy oil flow and oil-gas two-phase flow is estimated as P_{sb}. And it is believed the existence of foamy oil flow increases compressibility of oleic phase and contributes additional recovery efficiency compared with traditional solution gas drive process. The P_{sb} was estimated to be 2.1 MPa for test 2.

Meanwhile, the above analysis on 1D displacement characteristics is consistent with the observed foamy oil microscopic morphology, as shown in Figure 3(d). When the pressure is above the P_b of 5.1 MPa, there is no gas bubble. When the pressure is below the P_b and above the 2.1 MPa, gas bubbles emerge and highly disperse gradually. When the pressure drops below 2.1 MPa, gas bubbles begin to coalesce and finally continuous gas phase flow emerges.

In this way, for test 1, the pseudo bubble point pressure P_{sb} is determined to be 0.4 MPa. In the following parts, the results in test 1 and test 2 will be analysed and compared from three aspects: (1) foamy oil characteristics, (2) displacement characteristics, and (3) production performance.

3.2. Foamy Oil Characteristics. Compared with Figure 2(d) with Figure 3(d) and Table 4 with Table 5, it can be drawn that test 2 presents strong foam oil phenomenon, and bubbles are regular in shape, small, and highly dispersed. For test 1, the foamy oil behaviour emerges slowly and weakly. When pressure drops below the P_b and above 2.2 MPa, there presents a small number of bubbles dispersed in the oil phase, and the bubble diameter is large; when the pressure further drops below 2.2 MPa and P_{sb} of 0.4 MPa, the number of bubbles increases gradually. For example, when the pressure decreases from 1.7 MPa to 0.6 MPa, the number and density of bubbles increase from 24 and 5.32/cm^2 to 397 and 87.98/cm^2, respectively. However, it is still much lower than that in test 2.

3.3. Displacement Characteristics. When the system pressure is greater than P_b, the depressurization process of test 1 and test 2 both are in single-phase flow status and mainly depends on the elastic energy (Figures 2(c) and 3(c)). There is no dissolution gas released, and their displacement characteristics are similar. However, for test 2, the pressure at each pressure measuring point decreases linearly with time, and the decreasing rate is the same, as shown in Figure 3(c); for test 1, although the pressure at each pressure measuring point also decreases linearly with time, the decreasing rate is inconsistent. The closer to the outlet end, the lower the pressure, as shown in Figure 2(c). When the system pressure drops below P_b and above P_{sb}, for test 2, the system pressure could be effectively maintained due to the formation of a strong foam oil flow phenomenon. The pressures at the pressure measuring points P1 to P5 all also keep a linear decrease with time, although begin to deviate from the pressure value of the back-pressure valve. For test1, the inlet pressure is higher and the outlet pressure is lower, which indicates that the heavy oil mobility in deep reservoir is still very poor, and the foamy oil flow emerges mainly near the wellbore scope. When the system pressure is less than P_{sb}, for test 2, the formation pressure continues to decrease, and the pressure difference between the two ends further increases, but it is far less than that of test 1. Meanwhile, for test 1, the inlet pressure keeps high, the pressure difference increases gradually, and there exists a large displacement pressure.

3.4. Production Performance. When the pressure is greater than P_b, the production characteristics of test 1 and test 2 are similar, as shown in Figures 2(a) and 3(a). However, for test 2, the pressure difference between the formation pressure and saturation pressure is larger; thus, this stage of production lasts longer.

When the pressure is between P_b and the P_{sb}, compared with test 1, the cumulative oil production and recovery degree are higher, the foamy oil phenomenon is more obvious with longer duration and larger scope, the production pressure difference is less, and the heavy oil fluidity is stronger for test 2. Instead, in test 1, the pressure in the remote well-bore region remains high for a longer time, and the heavy oil fluidity in the deep reservoir was poor. Meanwhile, different from test 2, test 1 presents two-stage performance, an early stage and a late stage. In the early stage, it is difficult to form an effective foam oil flow by dispersing a small amount of dissolved gas in heavy oil. The oil production rate, cumulative oil production, and recovery degree increase slowly. In the later stage, the instantaneous gas oil ratio gradually increases, forming a weak foamy oil flow phenomenon, and the oil production rate, cumulative oil production, and recovery degree increase relatively rapidly (Figures 2(b) and 3(b)). The reasons for these differences are as follows: (1) Dissolved GOR has an important influence on the bubble nucleation process. In test 2, GOR is higher, and more dissolved gas is dispersed in heavy oil after depressurization to form a more obvious phenomenon of foamy oil. In addition, the higher the GOR is, the higher the critical gas saturation is, which is beneficial to reduce the gas mobility [11]. (2) In test 2, the asphaltene content is higher. Asphaltene is characterized with relatively stable molecular structure and larger molecular weight. It can be used as the bubble nucleation site, so it is conducive to the formation of foamy oil. In addition, asphaltene has the strongest interfacial activity in the crude oil components, which is beneficial to maintain the stability of the foamy oil [3]. (3) In test 2, the reservoir temperature is higher, the viscosity of heavy oil is lower, and the heavy oil mobility is stronger. Although the high temperature is not conducive to the stability of foamy oil, the temperature in the test 2 can still maintain the role of foamy oil. Consistent with previous studies, the phenomenon of strong foam oil occurred in the middle temperature range. In test 1, the reservoir temperature is low, the viscosity of heavy oil is large, and the fluidity is poor. Even if foamy oil emerges, it is difficult to flow and produce [6]. (4) In test 2, the reservoir pressure is higher, and the high pressure makes the oil-gas interfacial tension lower, which is favourable for

bubble nucleation to form foamy oil. Moreover, the foamy oil behaviour has a longer duration under high pressure [11].

When the pressure is lower than P_{sb}, for test 2, the oil production rate is greatly reduced, the cumulative oil production and recovery degree increase slowly, the foamy oil phenomenon gradually disappears, and the production performance gets worse. In addition, with a rapid increase of instantaneous gas oil ratio, free gas phase is formed, and bubbles are continuously generated, which follows the theory of progressive nucleation (Figures 3(a) and 3(b)). At this stage, test 1 is similar to test 2. However, the reduction degree of oil production rate, cumulative oil production, and recovery degree at this stage is lower than that in test 2, and it can still maintain a certain oil production capacity. In addition, the instantaneous gas oil ratio of test 1 increases rapidly in a short time and then decreases rapidly, following the instantaneous nucleation theory. The reasons for the above differences are as follows: (1) because the output between P_b and P_{sb} in test 1 is much lower than that in test 2, the remaining oil saturation in test 1 is higher. (2) In test 2, there is still a relatively larger displacement pressure.

For test 2, the cold recovery factor is 19.81%, the cumulative oil production is 30.95 g, the cumulative gas production is 1498 cm^3, and the maximum oil production rate is 0.34 g/min, which is 9.38%, 15.29 g, 1168.31 cm^3, and 0.10 g/min higher than that in test 1, respectively.

4. Conclusions

(1) Shallow heavy oil reservoirs in the Orinoco Belt present weaker foamy oil behaviour when compared with middepth heavy oils, due to such factors as reservoir pressure and temperature, solution GOR, and asphaltene content

(2) Cold production performance presents obvious three-stage features under the action of strong foamy oil displacement mechanism for middepth heavy oils. In the contrary, no such obvious production characteristics for shallow heavy oils are observed

(3) The stronger the foamy oil behaviour, the more favourable the cold production performance. Under the experimental condition, the primary recovery factor in middepth heavy oils is 9.38 percent point higher than which of shallow heavy oils

Data Availability

The raw/processed data required to reproduce these findings cannot be shared at this time as the data also forms part of an ongoing study.

Conflicts of Interest

The authors declare that there is no conflict of interest regarding the publication of this paper.

Acknowledgments

This research was funded by the China National Key Project (Project No.: 2016ZX05031).

References

[1] B. Maini, "Foamy oil flow in heavy oil prodution," *Journal of Canadian Petroleum Technology*, vol. 35, no. 6, pp. 21–24, 1996.

[2] B. B. Maini, H. K. Sarma, and A. E. George, "Significance of foamy-oil behaviour in primary production of heavy oils," *Journal of Canadian Petroleum Technology*, vol. 32, no. 9, pp. 45–50, 1993.

[3] X. Sun, Y. Zhang, Z. Gai, H. Zhao, G. Chen, and Z. Song, "Comprehensive experimental study of the interfacial stability of foamy oil and identification of the characteristic responsible for foamy oil formation," *Fuel*, vol. 238, pp. 514–525, 2019.

[4] X. Sun, Z. Song, L. Cai, Y. Zhang, and P. Li, "Phase behavior of heavy oil–solvent mixture systems under reservoir conditions," *Petroleum Science*, vol. 17, no. 6, pp. 1683–1698, 2020.

[5] M. Pooladi-Darvish and A. Firoozabadi, "Solution-gas drive in heavy oil reservoirs," *Journal of Canadian Petroleum Technology*, vol. 38, no. 4, pp. 54–61, 1999.

[6] Y. Zhang, B. B. Maini, and A. Chakma, "Effects of temperature on foamy oil flow in solution gas-drive in cold lake field," *Journal of Canadian Petroleum Technology*, vol. 38, no. 6, pp. 28–33, 1999.

[7] X. Chen and J. Qin, "Visualization study on foamy oil state," *Journal of Southeast Petroleum University (Science&Technology Edition)*, vol. 31, no. 6, pp. 126–130, 2009.

[8] O. Talabi and M. Pooladi-Darvish, "Effect of rate and viscosity on gas mobility during solution-gas drive in heavy oils," in *Paper SPE 84032 presented at the SPE Annual Technical Conference and Exhibition*, Denver, Colorado, U.S.A, 2003.

[9] X. Sun, J. Cai, X. Li, W. Zheng, T. Wang, and Y. Zhang, "Experimental investigation of a novel method for heavy oil recovery using supercritical multithermal fluid flooding," *Applied Thermal Engineering*, vol. 185, p. 116330, 2021.

[10] C. R. Satik, "A study of heavy oil solution gas drive for Hamaca Field: depletion studies and in-terpretations," in *Paper SPE 86967 presented at the SPE international Thermal Operations and Heavy Oil Symposium and Western Regional Meeting*, Bakersfield, California, U.S.A., 2004.

[11] X. Li, H. Chen, and Z. Yang, "Effect of GOR and temperature on gas mobility and recovery efficiency under solution-gas drive in heavy oils," in *Paper WHOC2015-319 Presented at the World Heavy Oil Congress Meeting*, Ddmonton, Alberta, Canada, 2015.